FIRST-CYCLE GRAIN WEATHERING PROCESSES: COMPOSITIONS AND TEXTURES OF SEA GLASS FROM PORT ALLEN, KAUAI, HAWAII

PATRICIA L. CORCORAN,[1] KATRINA PACKER,[1] AND MARK C. BIESINGER[2]

[1]Department of Earth Sciences, University of Western Ontario, London, Ontario, Canada N6A 5B7
[2]Surface Science Western, University of Western Ontario, London, Ontario, Canada N6A 5B7
e-mail: pcorcor@uwo.ca

ABSTRACT: Chemical and mechanical weathering textures on siliciclastic grains have provided important information concerning depositional processes and environments, yet understanding is limited by the multicycle origin of most sedimentary deposits. Sea glass grains sampled from a beach in Port Allen, Kauai, Hawaii, were analyzed for mechanical and chemical weathering features using scanning electron microscopy (SEM), energy dispersive X-ray (EDX) analysis, and X-ray photoelectron spectroscopy (XPS). As a result of a proximal dumping-ground source, the sea glass offers a unique opportunity to study first-cycle grain weathering processes in a moderate- to high-energy shoreline environment. Grain-size analysis indicates that the largest grains are located behind natural barriers, such as outcrops and boulders. The best-sorted samples are from the lower to middle foreshore environment, whereas moderately sorted deposits are located closer to the backshore where storm waves predominate. Although there is no preferred distribution of different-colored sea glass grains on the beach, non-frosted grains predominate over frosted varieties, suggesting constant input of fresh material.

Grain surface textures can be divided into mechanically dominated and chemically dominated weathering groups. Evidence of mechanical weathering is provided by conchoidal fractures, crescentic gouges, and straight grooves, whereas chemical weathering is indicated by c-shaped cracks, halite (salt) and silica precipitation, and solution pits. Combinations of these features demonstrate that both weathering processes work together to degrade the grains. XPS depth profiling of individual grains indicates that chemical weathering occurs at different grain depths, with leaching of sodium from the glass surfaces. This study provides a rare opportunity to relate grain compositions and textures with depositional and weathering processes, due to the first-cycle origin of the sea glass. The results show that using XPS and SEM techniques is a broadly applicable approach toward unraveling chemical and mechanical breakdown of sediment in beach environments.

INTRODUCTION

Previous workers have invoked specific depositional environments based on sand-grain surface textures (Krinsley and Doornkamp 1973; Mahaney 2002; Chakroun et al. 2009), with most studies focusing on the characteristics of glacial grains (Mahaney and Kalm 1995; Mahaney et al. 1996; Helland and Holmes 1997). However, using surface textures to determine depositional environments is problematic because microtextures may develop during erosion of the source rock (Krinsley and Doornkamp 1973; Mazzullo and Ritter 1991) and during multiple episodes of recycling. Sea glass represents excellent material with which to study the textural and chemical features of single-cycle, silica-rich beach sediment.

Sea glass, a naturally altered product of industrial glass, is locally abundant on beaches proximal to dumpsites, shipping lanes, or industrial areas (Lambert 2001; LaMotte 2004). Sourced from broken bottles and jars, fragments of sea glass are characterized by internal properties and external textures related to composition and weathering processes, respectively. Like natural sand and pebble beaches, sea-glass beaches are affected by transport and reworking by long shore drift currents, and ebb and flood currents related to tides and storm waves (LaMotte 2004). Each glass fragment exhibits surface textures and contains a specific major element and trace element composition, similar to grains of sand.

Using sea glass sampled from a beach at Port Allen, Kauai, the aim of this paper is to (1) describe and quantify different types of sea glass based on color and size, (2) elucidate the textural variations in glass fragments to determine the extent of exposure to mechanical and chemical weathering, (3) describe the prominent microtextures characteristic of a beach environment, and (4) determine which chemical elements in sea glass are most affected by weathering processes. No previous studies of this nature are known. Although sea-glass fragments on beaches are environmental waste, their use toward a better understanding of depositional and weathering processes represents a novel approach. The major advantage of studying sea glass lies in its first-cycle origin, which cannot be said for the majority of sand grains in the geological record.

GENERAL SETTING

The island of Kauai is located in the northwestern portion of the Hawaiian volcanic chain (Fig. 1A). The eight major islands are considered to have evolved or to be evolving through pre-shield, shield, post-shield, and rejuvenated stages as the Pacific plate has migrated to the west over a hotspot during the last ca. 40 My (Clague 1987; Clague and Dalrymple 1987; Clague and Dalrymple 1988; Blay and Siemers 2004). Rejuvenated-stage volcanism on Kauai ceased by approximately 0.52 Ma
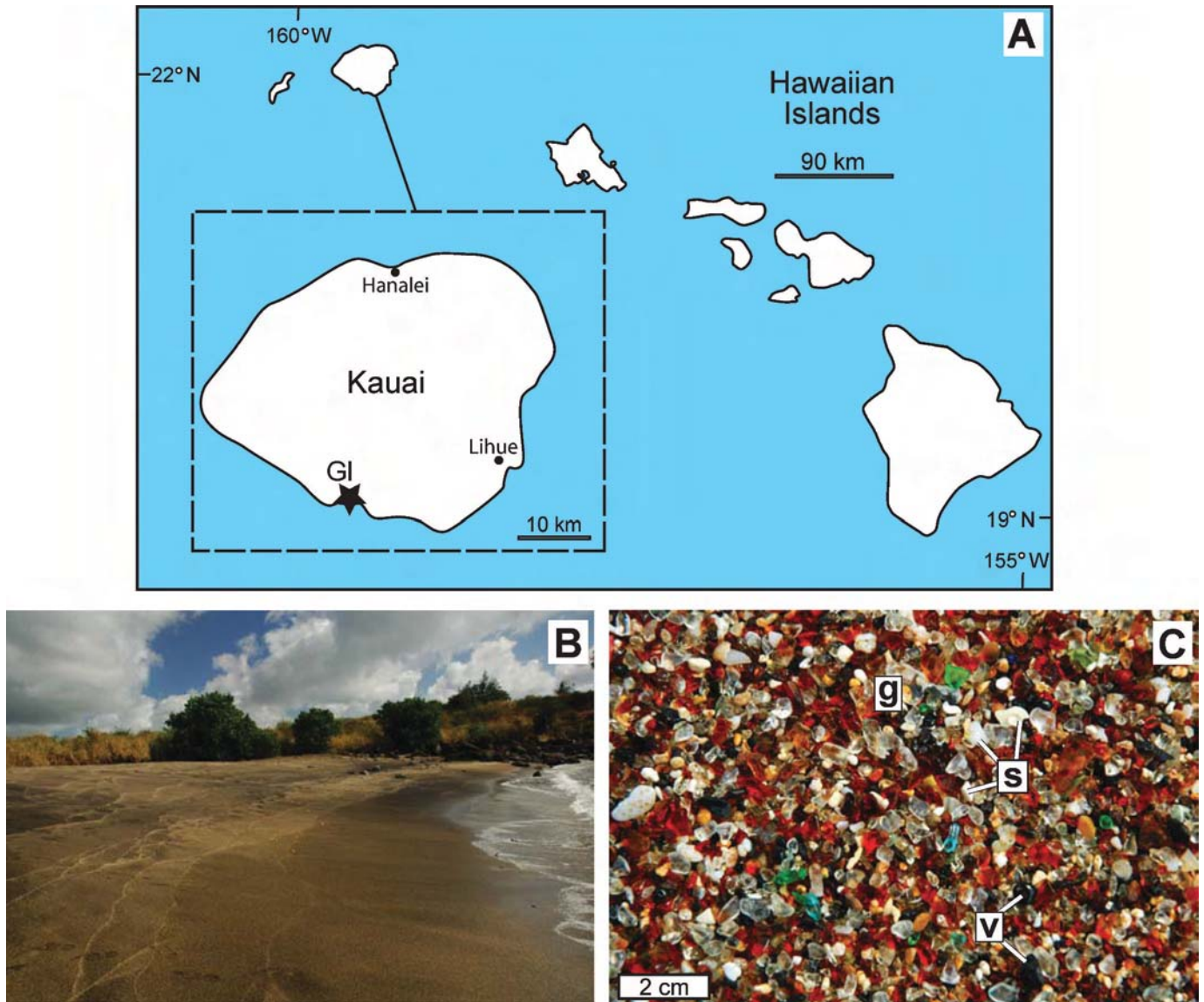
Fɪɢ. 1.—**A)** Map of the Hawaiian Islands illustrating the location of Kauai in the volcanic chain. Gl, Glass Beach at Port Allen. **B)** View of Glass Beach looking east. Field of view at bottom of photo is approximately 4 m. **C)** Close-up of grains constituting Glass Beach. Note the multicolored sea-glass grains (g), and the volcanic lithic (v) and shell (s) fragments.

(Clague and Dalrymple 1988) and is represented by the widespread distribution of the Koloa Volcanics over the eastern half of the island (Macdonald et al. 1960). Kauai is the most structurally complex and one of the oldest islands in the chain (Reiners et al. 1999), which accounts for the substantial erosional deposits constituting its numerous beaches.

The town of Port Allen, built on Koloa strata along Kauai's south coast, features a relatively small beach composed of sea-glass, volcanic lithic, and shell fragments (Figs. 1B, C). The sea glass is derived from a proximal dumping ground, where it originates as particles of broken bottles, jars, and windows that are removed and transported into the swash zone during storm events. The glass fragments are rounded through aqueous mechanical processes and are deposited on the beach. Interspersed volcanic lithic fragments are the eroded products of the Koloa Volcanics, which, in the area of Port Allen, are mainly olivine

basalt and nepheline basalt flows (Macdonald et al. 1960; Sherrod et al. 2007). Shell fragments in the beach sediment include broken shells, foraminifera, and coral.

The climate of the Hawaiian Islands is governed largely by the prevailing northeast trade winds, which are interrupted occasionally by severe storms during the winter months (Macdonald et al. 1960). Ocean waves that alter the shoreline of Kauai are brought to the island by the northeast trade winds, Kona winds, and the effects of North and South Pacific Ocean storms (Blay and Siemers 2004). The relatively mild climate on Kauai is in part attributed to modulation of the trade winds by the mountainous interior, which in turn affects the strength and direction of ocean currents (Xie et al. 2001; Yang et al. 2008). The ocean currents in the Hawaiian chain flow in an anticyclonic direction, or clockwise motion, around each island (Patzert and Wyrtki 1974). Transport, reworking, and deposition of sediment along beaches occur by longshore
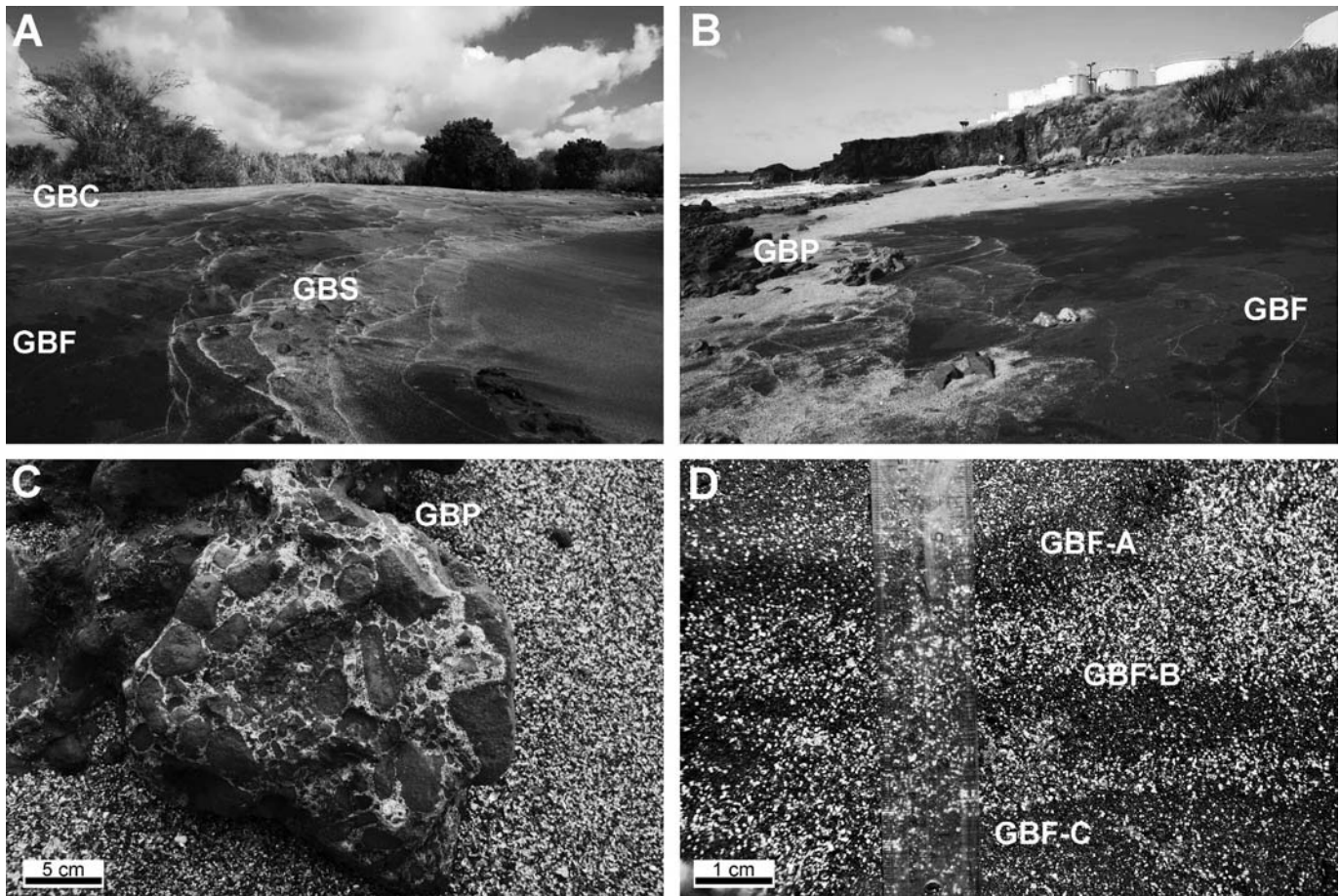
FIG. 2.—Sample locations on Glass Beach. **A**, **B)** Locations of samples GBC (foreshore–backshore), GBF (middle foreshore), GBS and GBP (lower foreshore). Field of view at bottom of photos is approximately 4 m. **C)** Close-up location of sample GBP sands behind an outcrop. D) Site from where samples GBS-A, -B, and -C were collected. Note the laminae with inverse size grading and abundance of volcanic lithic fragments (dark grains) within the medium-grained fraction.

drift and ebb and flood currents, which collectively govern the distribution of sea glass in the study area.

DATA COLLECTION AND GRAIN SIZE DISTRIBUTION

Beach grains, including sea-glass, lithic–volcanic, and shell fragments, were sampled from four sites: (1) along the strandline in the lower foreshore (GBS), (2) behind an outcrop in the lower foreshore (GBP), (3) from coarse-grained material at the foreshore–backshore transition zone (GBC) and (4) from fine-grained material in the middle foreshore (GBF; Fig. 2A–C). A small trench was dug at GBF, where three samples were collected at different depths of < 2.0 cm (GBF-A), 7.5 cm (GBF-B), and 12.5 cm (GBF-C; Fig. 2D). Each sample was sieved for 2 minutes using an AS 200 digital shaker with stainless steel sieves. The very coarse-grained samples GBP, GBS, and GBC were processed using sieve diameters of 5.6 mm to 0.3 mm, whereas the coarse-grained samples GBF-A, GBF-B, and GBF-C, were separated into diameters of 2.36 mm to 0.15 mm. Each separate was weighed to determine grain-size frequency distribution. The samples range from medium sand (GBF-A) to granules (GBP) and are moderately (GBC) to very well sorted (GBF-C) (Table 1).

GRAIN TYPE AND COLOR DISTRIBUTION

Grain type and color distribution were determined using the ribbon counting method (cf. Middleton et al. 1985) on four hundred grains from nine selected separates, which included the very coarse-grained GBP

(2.36–4.0 mm; 1.46–2.36 mm; 0.85–1.46 mm), GBS (1.46–2.36 mm; 0.85–1.46 mm), and GBC (0.85–1.46 mm), and the coarse-grained GBF-A (0.85–1.46 mm), GBF-B (0.85–1.46 mm) and GBF-C (0.85–1.46 mm). The grains were divided into (1) green non-frosted, (2) green frosted, (3) white non-frosted, (4) white frosted, (5) brown non-frosted, and (6) brown frosted glass, in addition to (7) volcanic lithic and (8) shell fragments. Although blue, purple, red, and orange glass grains were identified, they were too rare in each sample to include in the classification scheme.

The majority of sample GBP contains sea glass (58%), with secondary non-glass components of skeletal (23%) and volcanic lithic (19%) fragments (Fig. 3). The sea-glass constituent is represented mainly by brown and white non-frosted and frosted grains. In contrast, sample GBS is composed of more volcanic lithic and skeletal fragments (54%) than sea glass (46%), and compared to GBP, contains a higher percentage of non-frosted than frosted types (Fig. 3). White and brown colors predominate. Volcanic lithic and shell fragments (52%) are in almost equal proportion to sea glass (48%) in sample GBC. Similarly to samples GBP and GBS, brown and white glass grains are common, but as in GBS, non-frosted varieties predominate. All separates from the very coarse-grained samples contain a secondary component of green glass.

The coarse-grained separates from samples GBF–A, GBF–B, and GBF–C are composed of significantly less sea glass than their very coarse-grained counterparts (Fig. 3). Sea glass constitutes 9% of sample GBF-A, with only non-frosted brown, white, and green varieties. Similarly, GBF–

TABLE 1.— *Grain-size analysis for bulk samples.*

Sample #	Grain Size	Sorting
GBP	Very coarse sand to granules	Well sorted
GBC	Very coarse sand	Moderately sorted
GBS	Very coarse sand	Well sorted
GBF-A	Medium sand	Well sorted
GBF-B	Coarse sand	Well sorted
GBF-C	Coarse sand	Very well sorted

B contains 8% sea glass, which is predominantly non-frosted. White, brown, and green colors are common.

GBF–C, compared with the other coarse-grained samples, contains the greatest proportion of sea glass (18%), which is primarily non-frosted (Fig. 3). Only white and brown colors characterize sample GBF–C.

TEXTURAL ANALYSIS

Sixty-two sea-glass grains were examined using a Nikon SMZ 1500 optical microscope and a Hitachi S-4500 field emission scanning electron microscope (SEM) at Surface Science Western, University of Western Ontario. The samples chosen ranged from grain sizes of 0.85–2.36 mm

and included (1) medium green, non-frosted, (2) forest green, non-frosted, (3) forest green, frosted, (4) medium blue, non-frosted, (5) light blue, non-frosted, (6) aqua blue, non-frosted, (7) purple, non-frosted, (8) red, non-frosted, (9) orange, non-frosted, (10) brown, non-frosted, (11) brown, frosted, (12) white, non-frosted, and (13) white, frosted grains. To prevent sample charging during SEM analyses, 47 of the samples were coated with gold, and the red non-frosted and orange non-frosted samples, were coated with carbon. SEM imaging was conducted at electron accelerating voltages of 5 and 15 kV with a sample tilt of 30 degrees.

Sea-glass grains between 1.4 mm and 2.36 mm in size were examined for surface textures typical of mechanical and chemical weathering processes (Fig. 4). Predominant mechanical weathering features include conchoidal fractures, crescentic gouges, and straight grooves (Fig. 5A–C). Chemical weathering textures are represented primarily by halite (salt) and silica precipitation, and solution pits (Fig. 5D, E). The most abundant textures are c-shaped cracks (Fig. 5C, F), which surficially resemble the v-shaped cracks described by Krinsley and Doornkamp (1973). V-shaped patterns in natural sediment grains have been interpreted as percussion marks that form during grain to grain interaction in high-energy environments. In contrast, c-shaped cracks in sea glass have been attributed to hydration, wherein the soda in the glass is replaced by hydrogen ions derived from the seawater (LaMotte 2004). The resultant sodium hydroxide becomes leached from the glass surface,
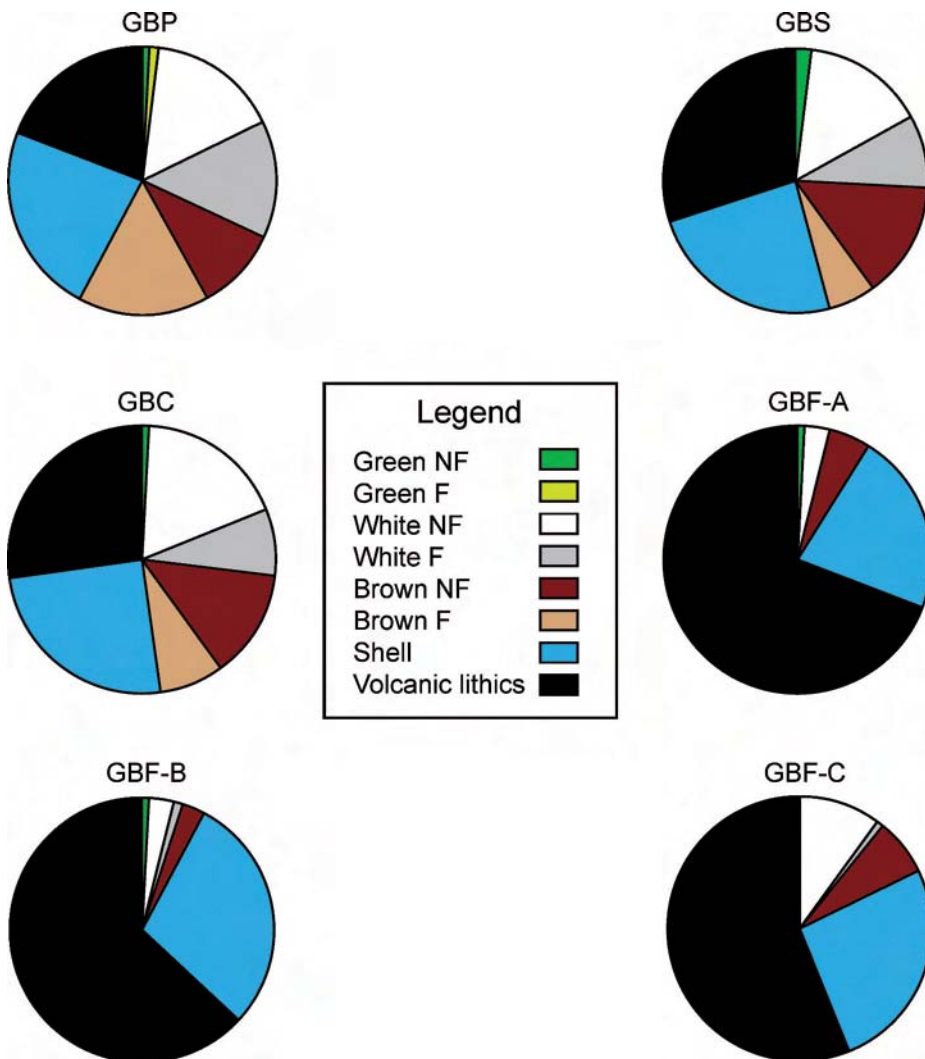

FIG. 3.—Abundances of different grain types, derived from point counting. Note how volcanic lithic grains are abundant in the GBF sample series. In all samples, except GBP, non-frosted sea glass (NF) predominates over frosted (F) varieties.
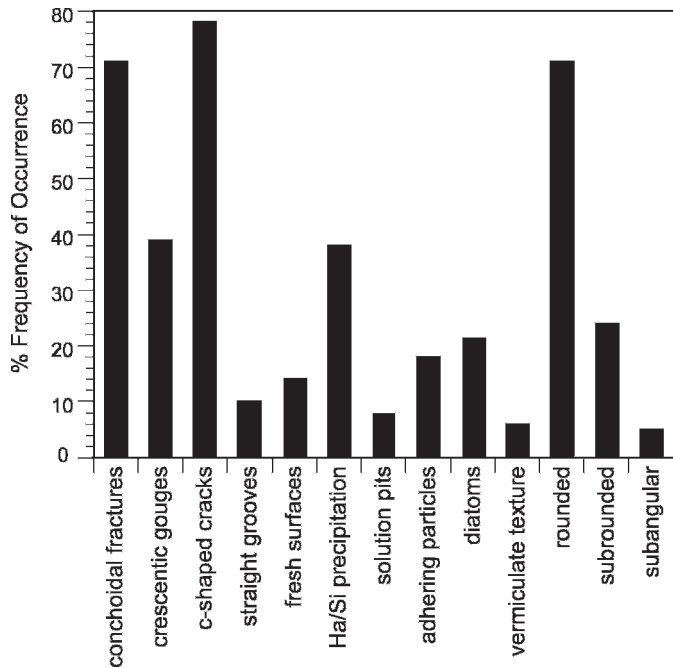
Fig. 4.—Bar graph illustrating the frequency of occurrence (percentage) of different mechanical and chemical weathering textures on sea glass. Note the abundance of conchoidal fractures, c-shaped cracks, and rounded grains.

leaving a frosted appearance. Comparisons made between frosted and non-frosted sea glass illustrate that frosting, roundness, and abundant c-shaped cracks occur together. There was no correlation between color and type or density of mechanically imparted features. Allochthonous materials, including adhering particles and diatoms, are concentrated in solution pits and along fractures within which silica precipitation has occurred (Fig. 5G). Vermiculate patterns are locally preserved on three grains (Fig. 5H). Sea-glass fragments with fresh surfaces (low relief) are interpreted as relatively young grains, based on the absence of mechanical and chemical weathering textures. The low-relief grains are predominantly subrounded to angular.

COMPOSITIONAL ANALYSIS

Energy dispersive X-ray (EDX) analysis (15 kV) was conducted to determine the proportions of selected major and trace elements in 12 representative sea-glass grains using a Phoenix EDAX system attached to the Hitachi S-4500 SEM at Surface Science Western. The detection limit of approximately 0.1 to 0.5 weight percent (wt%, element dependent) restricted the analyses to the major elements, O, Na, Mg, Al, Si, Cl, K, Ca, Zn, Fe, and Mn. The results indicate some major element variability between different grain colors (Table 2). Orange and red sea glass contain greater O wt% than green, blue, brown, and white glass, and lower Si wt% than all other grains. The frosted grains contain greater amounts of Cl than the non-frosted varieties. However, the greatest variability between colors is displayed in the transition metals Mn, Fe, and Zn. Aqua blue

and normal blue are the only non-frosted grains containing detectable Fe, whereas Mn was detected in the purple grain, and Zn was detected in the orange grain only (Table 2). Glass is manufactured with a basic composition of 75% silica sand, 15% soda, and 10% lime, but the percentage of each of the primary elements varies (La Motte 2004). In order to obtain specific colors, transition metals, such as Ti, V, Cr, Mn, Fe, and Co, and the rare earth elements (REE) are added (Carter and Norton 2007). Excess Mn is often used to create violet hues (LaMotte 2004; Carter and Norton 2007), whereas the Fe in the normal and aqua blue grains may be consistent with the presence of iron oxide in the original sand. It is unclear whether the Zn detected in the orange grain is responsible for its rare color. There is some mention in the literature of the addition of 2–8% ZnO and sulfur (creating ZnS) to glass to increase its opacity. The ZnS could then react with trace amounts of iron oxide impurities in the glass to produce ferric sulfide. This can give the glass a "yellow-brown" appearance (Fridman 1962).

More significantly, element variations occur between single-colored frosted and non-frosted sea glass. A comparison of non-frosted and frosted white grains indicates an increase in O, Na, and Al, a decrease in Mg, Si, K, and Ca, and an appearance of Cl and Fe in the frosted grain (Fig. 6).

Compositional results determined from X-ray photoelectron spectroscopy (XPS) depth profiling displayed variable element proportions dependent on location below the surface of each grain. Depth profiling of a white frosted and a brown frosted grain was conducted using a Kratos Axis Ultra X-ray photoelectron spectrometer (XPS) using monochromatic Al $K\alpha$ x-rays (1486.7 eV). The Kratos charge-neutralization system was used for all samples analyzed. In the XPS depth profiling experiment, a survey scan analysis is first taken (pass energy 160 eV, analyses area of 300 microns $\times$ 700 microns). Following the survey scan, a 3 mm $\times$ 3 mm surface area is ablated using a 4 kV Ar^+ ion beam for a specific time period (sputter rate of 1.4 nm/ min based on an Al_2O_3/Al standard). At this new depth, another survey scan spectrum is obtained. These steps are repeated, profiling the amount of each element present into the bulk of the glass substrate.

The analyzed white frosted grain contained Cu in the outer 13 nm, Cl in the outer 140 nm, and Fe in the outer 190 nm (Fig. 7A, B). At a depth of approximately 190 nm below the surface, the amount of primary elements increased relatively uniformly to close to bulk concentrations as the amount of surface element (in particular, carbon) decreased to nil. Bulk levels as determined by XPS for this glass are as follows: O (60.0 At. %), Na (3.0 At. %), Ca (6.6 At. %), Si (22.5 At. %), Al (1.4 At. %), K (0.9 At. %), Mg (2.7 At. %), C (1.9 At. %), and N (0.9 At. %). An examination of Na:O and Na:Si ratios from the surface to bulk shows a depletion of Na at the surface to a depth of approximately 30 nm. A similar examination of Ca:O and Ca:Si ratios, Mg:O and Mg:Si ratios, and K:O and K:Si ratios shows negligible depletion of Ca, Mg, or K at the surface of the glass. Small amounts of carbon persisted throughout the profile, even at 600 nm depths, though this is probably due to absorbed (adventitious) carbon from the vacuum of the instrument during analysis. Nitrogen decreased (2.4 At. % to 0.9 At. %) but was still detected after an etch time of 25,000 seconds (> 600 nm). The elemental quantity of K remained relatively unchanged throughout the profile (1.1 At. % to 0.9 At. %).

$\rightarrow$

Fig. 5.—SEM images of sea-glass surface textures. **A)** Conchoidal fractures (CF) on a relatively fresh grain with subrounded edges. **B)** Crescentic gouge (CG) on a frosted grain. **C)** Straight groove (SG) and c-shaped cracks (C) on a rounded, frosted grain. **D)** Halite (H) precipitation on a subrounded grain. **E)** Solution pits (P) on a rounded, frosted grain. **F)** C-shaped cracks (C) formed by chemical weathering on a rounded, frosted grain. **G)** Diatoms (D) and silica precipitation (SP) within a crack on a non-frosted grain. **H)** Vermiculate texture (V) resembling borings on a non-frosted grain.
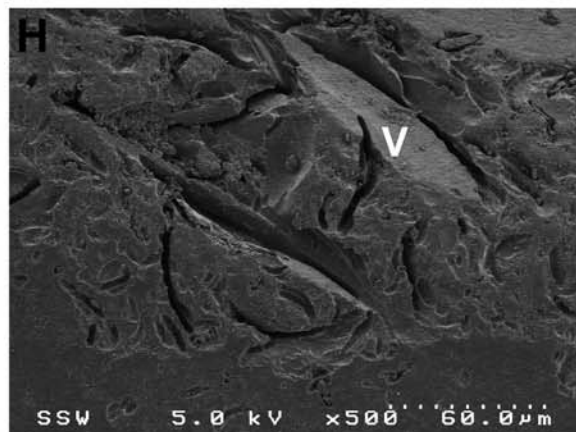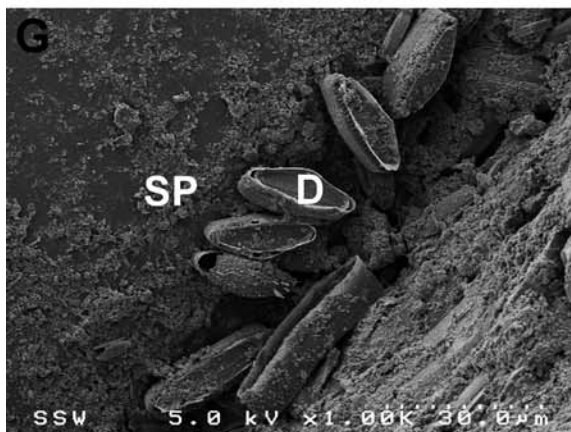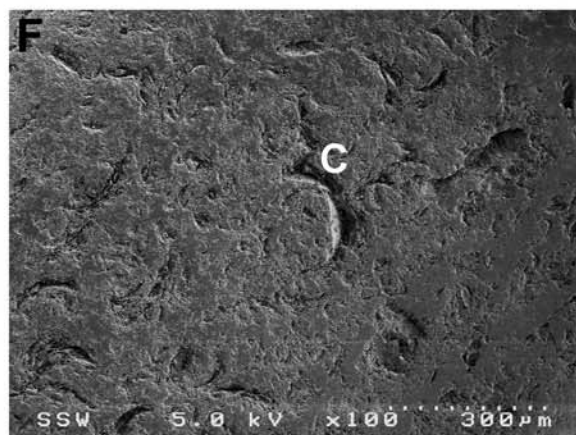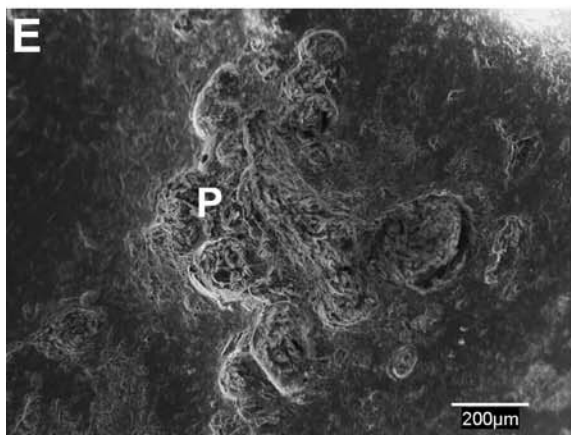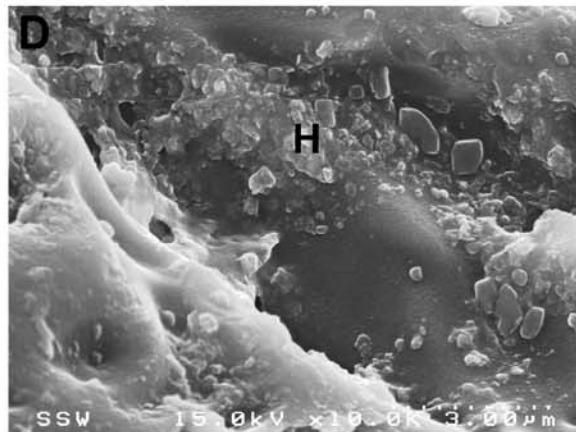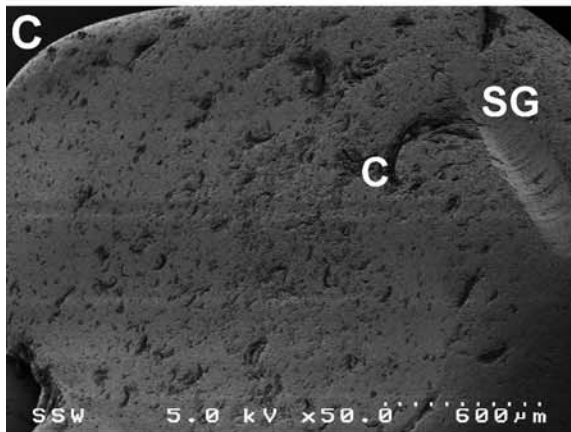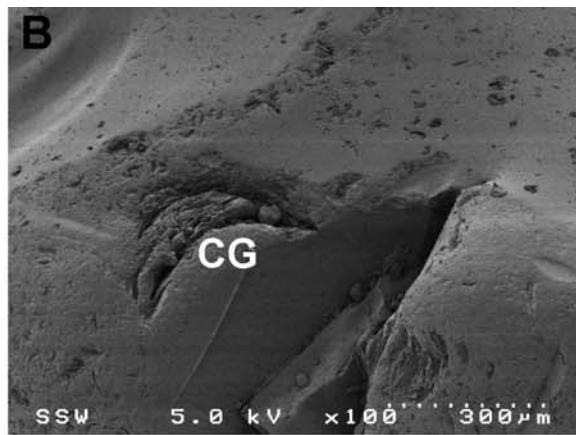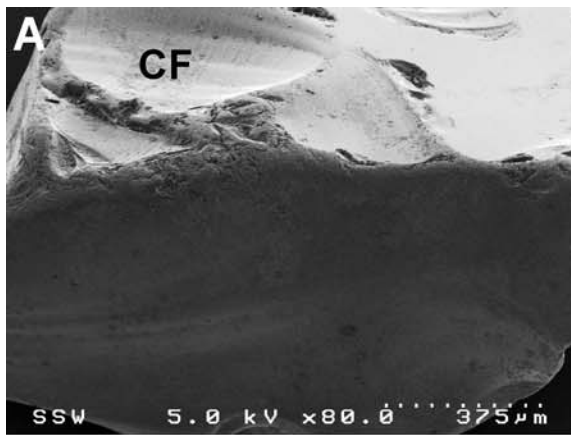
TABLE 2.— *SEM-EDX analysis in wt % of 12 representative sea-glass grains.*

Element (wt%)	Orange NF	Red NF	Medium Green NF	Forest Green NF	Medium Blue NF	Light Blue NF	Purple NF	Aqua Blue NF	Brown NF	White NF	Brown F	White F
O	43.1	45.1	27.5	39.6	35.1	38.6	44.5	34.6	28.3	20.6	25.2	36.9
Na	10.6	12.1	7.4	8.1	11.1	12.1	4.7	10.1	11.4	9.2	7.4	11.1
Mg	0.0	0.0	1.1	2.2	1.3	3.7	0.0	0.0	0.0	3.1	0.9	1.9
Al	0.9	1.9	2.6	1.9	2.2	2.0	2.2	5.2	5.0	2.3	3.5	3.1
Si	36.5	35.1	50.0	37.1	43.3	38.8	43.0	40.1	45.7	54.9	48.3	38.0
Cl	0.0	0.5	0.0	0.5	0.0	0.7	0.7	0.7	0.0	0.0	1.3	1.7
K	4.2	0.5	1.7	1.0	0.5	0.0	1.1	2.5	1.7	1.7	3.7	0.7
Ca	1.5	4.8	10.0	9.7	5.9	4.2	2.7	5.8	7.9	8.2	9.5	5.8
Zn	3.2	0.0	0.0	0.0	0.0	0.0	0.0	0.0	0.0	0.0	0.0	0.0
Fe	0.0	0.0	0.0	0.0	0.7	0.0	0.0	0.8	0.0	0.0	0.0	0.8
Mn	0.0	0.0	0.0	0.0	0.0	0.0	1.1	0.0	0.0	0.0	0.0	0.0
Total	100	100	100.3	100.1	100.1	100.1	100	99.8	100	100	99.8	100

The analyzed brown frosted grain contained small amounts of K, Fe, and N in the outer 50 nm and minor Cl in the outer 7 nm of the sample (Fig. 8A, B). Bulk levels as determined by XPS for this glass fragment are as follows: O (65.6 At. %), Na (3.1 At. %), Ca (7.9 At. %), Si (20.0 At. %), Al (0.9 At. %), Mg (2.7 At. %), and C (0.9 At. %). Examination of Na:O and Na:Si ratios from the surface to bulk shows a depletion of Na at the surface to a depth of approximately 125 nm, which is significantly deeper than in the white glass fragment. The Ca:O and Ca:Si ratios show depletion of Ca from the surface to a depth of approximately 20 nm. In contrast, Mg:O and Mg:Si ratios display slightly elevated levels of Mg at the surface compared to the bulk. K was present at the surface to a depth of approximately 50 nm but was not detected in the bulk of the glass fragment. Chlorine and Fe, which were detected in the white frosted grain using SEM-EDX analysis, were not detected by XPS analysis below certain depths in either the white or brown frosted grains, indicating that these elements are present only at the surface.
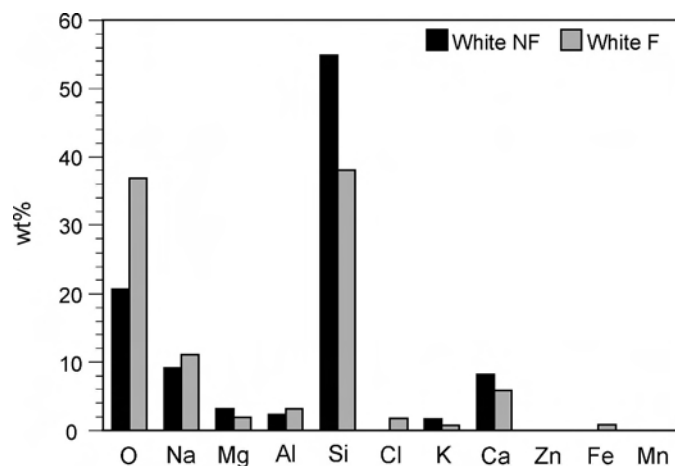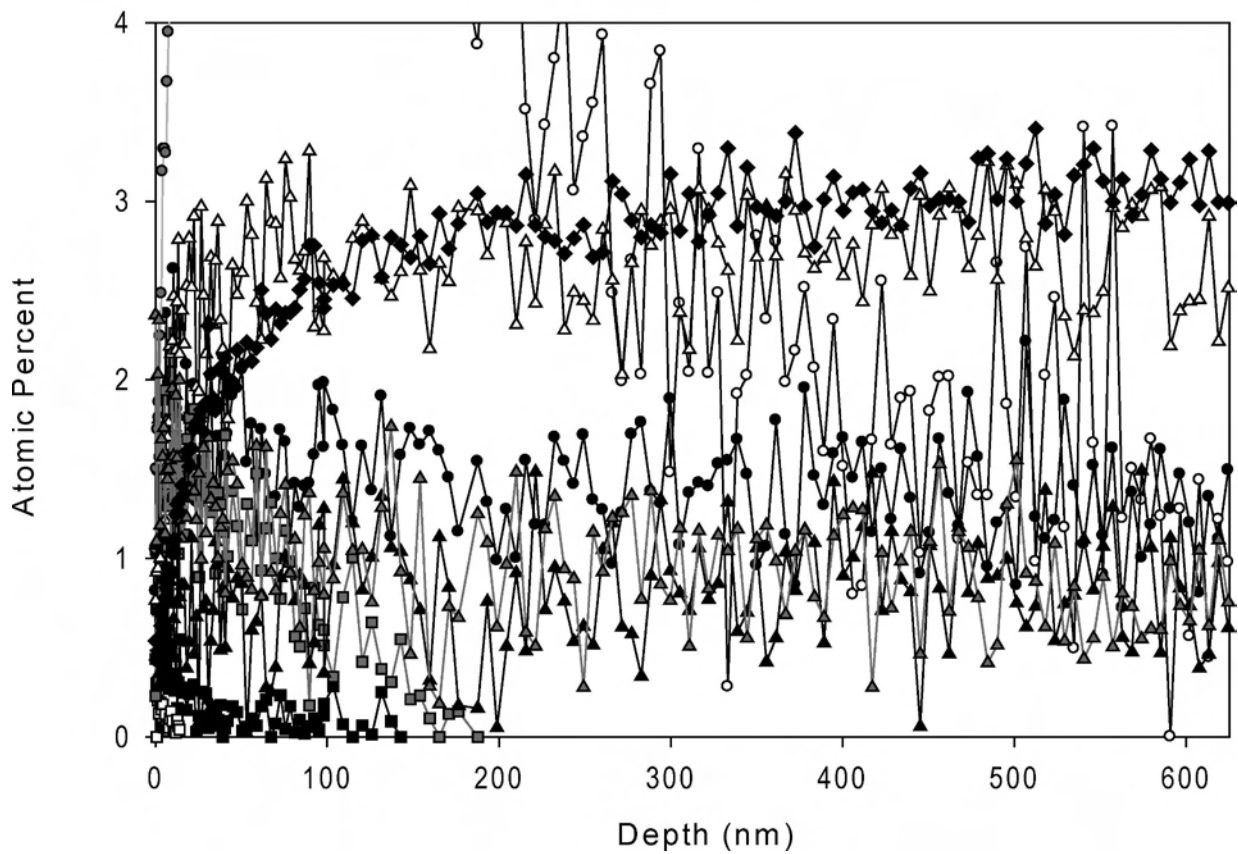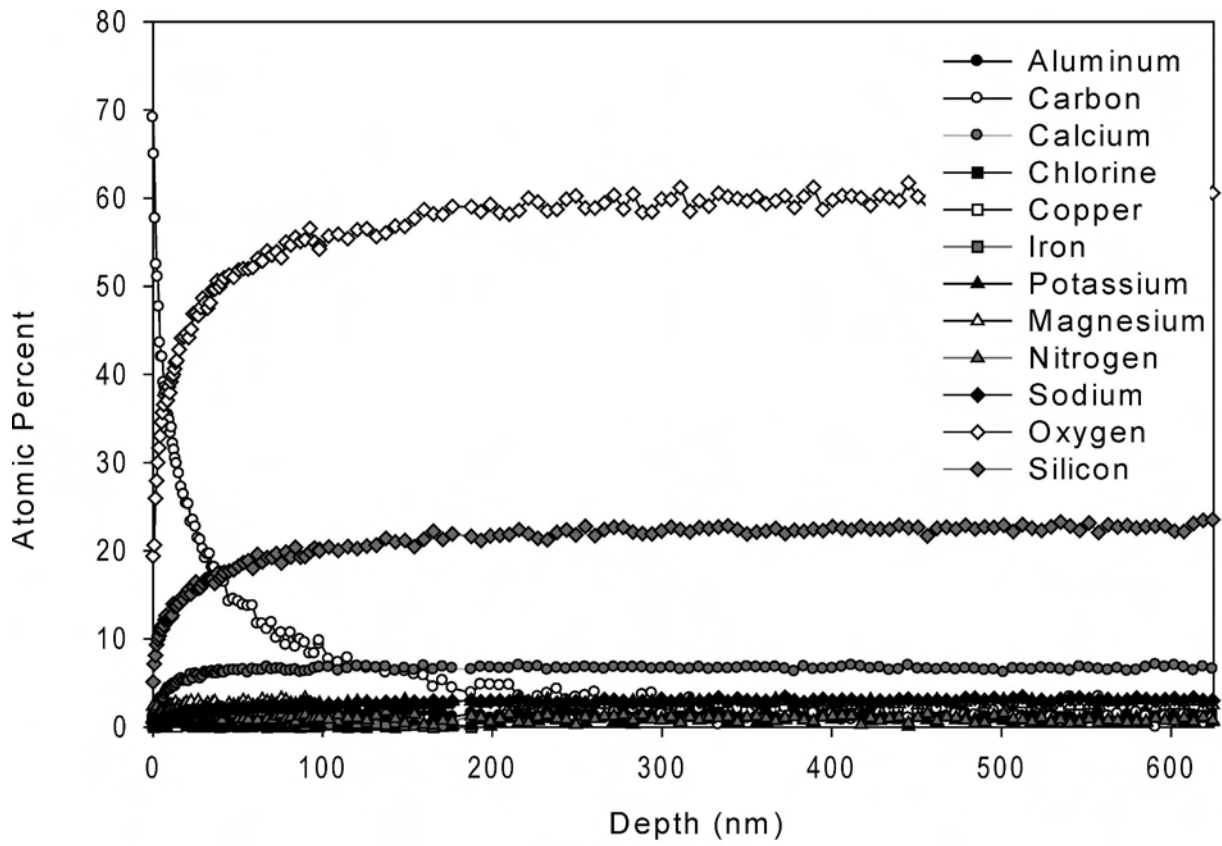

FIG. 6.—Bar graph comparing the weight percent (wt%) of each major element in white frosted and white non-frosted sea glass based on SEM-EDX analysis. Note how the percentages of O, Na, Al, Cl, and Fe are greater for the frosted glass.

DISCUSSION

Distribution of Sea Glass on the Beach

The deposits on Glass Beach are generally well sorted. The moderate sorting of sample GBC is a function of its location in the foreshore–backshore transition zone. The upper foreshore to backshore region receives sediment intermittently, and the degree of reworking is much less than that occurring in the swash zone. Samples GBP, GBS, and GBF-A, B, and C were collected from the middle to lower foreshore environment (Fig. 2A–C) where wave and current reworking predominates, thus increasing the degree of sorting. Parallel lamination with reverse size grading at sampling site GBF (Fig. 2D) is typical of foreshore environments and represents grain segregation in bed flow during swash–backwash processes (Clifton 1969). The laminae are composed of basal medium-grained to upper coarse-grained couplets, accounting for the variations in grain size between samples GBF-A (medium sand) and GBF-B and -C (coarse sand). Sample GBP is composed of very coarse sand to granules, which reflects its location behind an outcrop. The outcrop acts as a barrier restricting tractional transport of coarse grains back to the ocean during backwash flow.

Point counting of different-colored sea glass indicates that color sorting does not occur (Fig. 4), even though certain elements added during the glass-making process to create specific colors have higher relative densities than others. In most samples, non-frosted grains predominate over frosted types, consistent with a steady input of fresh glass to the area. Based on personal observations, sea-glass collectors and tourists remove hundreds to thousands of fragments from the beach in a single day, but a renewed supply of sea glass is deposited following the next high tide. Rapid diminution of sand-size fragments into finer grain sizes was considered a potential cause of the higher non-frosted to frosted grain ratios in the coarse-grained deposits, but there are even fewer frosted grains in the medium-grained (GBF-A) than in the granular (GBP) sample. Sample GBP is the only location where the frosted component is greater than (brown) or almost equal to (white) the non-frosted component (Fig. 4). Inasmuch as frosting is attributed to chemical weathering (LaMotte 2004), the results suggest that the sea glass of GBP experienced longer sediment residence times behind the outcrop than the grains that were exposed to the open ocean. Based on the higher abundances of volcanic lithics relative to sea-glass grains in GBF-A, -B, and -C (Figs. 2B–D, 4), it could be inferred that the greatest amount of

→

FIG. 7.—XPS depth profile of the surface of a white frosted grain (top: full profile, bottom: expanded view to show low-level constituents). Key is the same in upper and lower figures. Note the depletion of Na towards the surface of the grain.

swash–backwash flow occurred in the middle foreshore compared with areas in the lower foreshore (GBS and GBP) and foreshore to backshore transition zone (GBC). All three samples from the trench at GBF were in part collected from the basal, volcanic–lithic-rich divisions of the medium-grained and coarse grained couplets (Fig. 2D).

Implications of Sea Glass Textures

Quartz grain surface textures have long been considered useful for interpreting depositional environments (Krinsley and Doornkamp 1973; Margolis and Krinsley 1974; Mahaney 2002). Grains of glacial (Mahaney and Kalm 1995; Helland and Holmes 1997), eolian (Margolis and Krinsley 1971), littoral (Blackwelder and Pilkey 1972; Moral Cardonna et al. 1997), and mixed (Hodel et al. 1988; Damiani et al. 2006) origin have been proposed based on combinations of specific mechanical and chemical weathering features. Although the chemistry of soda-lime (bottle) sea glass differs from pure quartz (approximately 75% silica sand, 15% sodium bicarbonate, 10% calcium oxide; LaMotte 2004), its relatively high percentage of SiO_2, amorphous nature, and specific gravity (approximately 2.5) results in mechanically-imparted surface features that are comparable to quartz. The surface microtextures on sea glass from Port Allen are comparable to quartz grains of littoral origin, with some exceptions. Conchoidal fractures and straight grooves, which are common surface textures on sea glass from Port Allen (Fig. 5A), have been considered indicators of relict (directly from source), glacial and littoral environments (Blackwelder and Pilkey 1972; Krinsley and Doornkamp 1973; Hodel et al. 1988; Damiani et al. 2006). High-energy subaqueous processes have been inferred for both conchoidal fractures and straight grooves (cracks) on quartz grains, where uniform compression between grains and high abrasion levels occur (Margolis and Krinsley 1974). Mechanically imparted surface defects and fractures would have been formed from impacts by volcanic lithic fragments which contain minerals with equal or higher relative hardness (olivine 6.5–7, pyroxene 5–6, plagioclase 6) than bottle-derived sea glass (hardness of 5–6). The v-shaped pits that preferentially develop in medium- to high-energy subaqueous environments due to abrasion (Krinsley and Doornkamp 1973; Margolis and Krinsley 1974; Hodel et al. 1988) are noticeably absent from the Port Allen grains. Margolis and Kennett (1971) showed that abundant v-shaped pits can result from cumulative abrasion over multiple transport cycles and recycling, which could explain why the first-cycle sea glass sands at Port Allen do not contain these features even though they were deposited in a beach environment. Other common surface textures on the sea glass are crescentic gouges (Fig. 5B), which have mainly been attributed to glacial action (Mahaney et al. 1988). If these gouges are comparable to the curved scratches of Margolis and Krinsley (1974), they could also form in medium- to high-energy subaqueous environments. The problem in environmental interpretation then becomes one of terminology.

The most abundant textures in this study are c-shaped cracks (Fig. 5F), which have not been reported previously from the literature, suggesting that these microtextures develop exclusively on sea glass as a result of reactions between hydrogen ions and sodium ions. The association of c-shaped cracks, frosting, and roundness suggests that chemical weathering has removed or modified most of the mechanical weathering features. Adhering particles, which coat 18% of the sea glass surfaces, have been reported from grains of glacial origin (Mahaney and Kalm 1995; Helland and Holmes 1997). However, unlike particles on glacially derived grains,

the majority of particles on the sea-glass samples are composed of crystals of NaCl (Fig. 5D) derived from the seawater. Diatoms identified in fractures and solution pits (Fig. 5E, G) were concentrated in low-relief grain features post-mortem. Dissolution etching and solution pits (Fig. 5C, E) indicate extended exposure to alkaline seawater in which the precipitation of calcium carbonate accompanies dissolution of quartz (Friedman et al. 1976). Alternatively, the pits could have resulted from preferential dissolution of soda and lime in the glass (LaMotte 2004). There is no relationship between the density of chemical-weathering textures and location on the beach, indicating that the grains are continually being reworked. Rare vermiculate patterns resemble borings, which could indicate a possible biological contribution to sea-glass degradation.

If the deposits at Glass Beach were lithified, the predominant conchoidal fractures, crescentic gouges, and adhering particles on the grains could result in a glacial-origin interpretation, but the absence of breakage blocks, steps, and striations, in addition to the subrounded to rounded forms of the grains, are more consistent with littoral processes.

Implications of Sea Glass Compositions

The EDX analyses conducted on different sea-glass grains confirm that slight chemical variations result in color differences. In terms of durability, the lower percentage of Si in red and orange sea glass, and higher Mn in the purple grain may result in greater chemical and mechanical breakdown than of green, brown, and white fragments. The rarity of orange, red, and purple sea glass on beaches globally (LaMotte 2004) is mainly a function of lower production rates.

The XPS depth profiles show that leaching of sodium from the glass surfaces is occurring. This is a well-known phenomenon (e.g., Doremus 1975) that varies in severity with glass composition, solution chemistry, and pH. The chemistry of natural sea water around the study area is assumed to be generally constant, owing to the low temperature differences throughout the year in addition to the absence of freeze–thaw cycles, freshwater input, and high evaporation rates. Therefore, the composition of the glass is the dominant factor in sodium leaching. Current theories of leaching mechanisms are based on ion-exchange models involving the interdiffusion of H^+ and alkali ions (Kaneko 1985). The competing processes of chemical leaching and continual mechanical weathering probably keeps the observed depth of leaching shallow. The process amounts to a moving boundary-value problem in which the weathered surface is continually being "swept away" by physical abrasion, while chemical weathering, and hydration of the industrial glass surfaces occurs. This leads to a volume change of the surface material and a concomitant build up of near-surface strain energy that makes the surface material more susceptible to removal by abrasion and surficial weathering. Similar processes are described for other geologic systems such as the spheroidal weathering and denudation of saprolite (e.g., Fletcher et al. 2006; Lebdeva et al. 2007).

CONCLUSIONS

The abundance of chemical and mechanical weathering textures on first-cycle sea-glass grains provides a unique opportunity to study the features that develop in medium- to high-energy subaqueous environments. Surface textures illustrate the relative controls of the two weathering types, and the role each plays in beach grain degradation. Mechanical-weathering textures, which include conchoidal fractures,

→

FIG. 8.—XPS depth profile of the surface of a brown frosted grain (top: full profile, bottom: expanded view to show low-level constituents). Key is the same in upper and lower figures. Note the depletion of Na towards the surface of the grain.
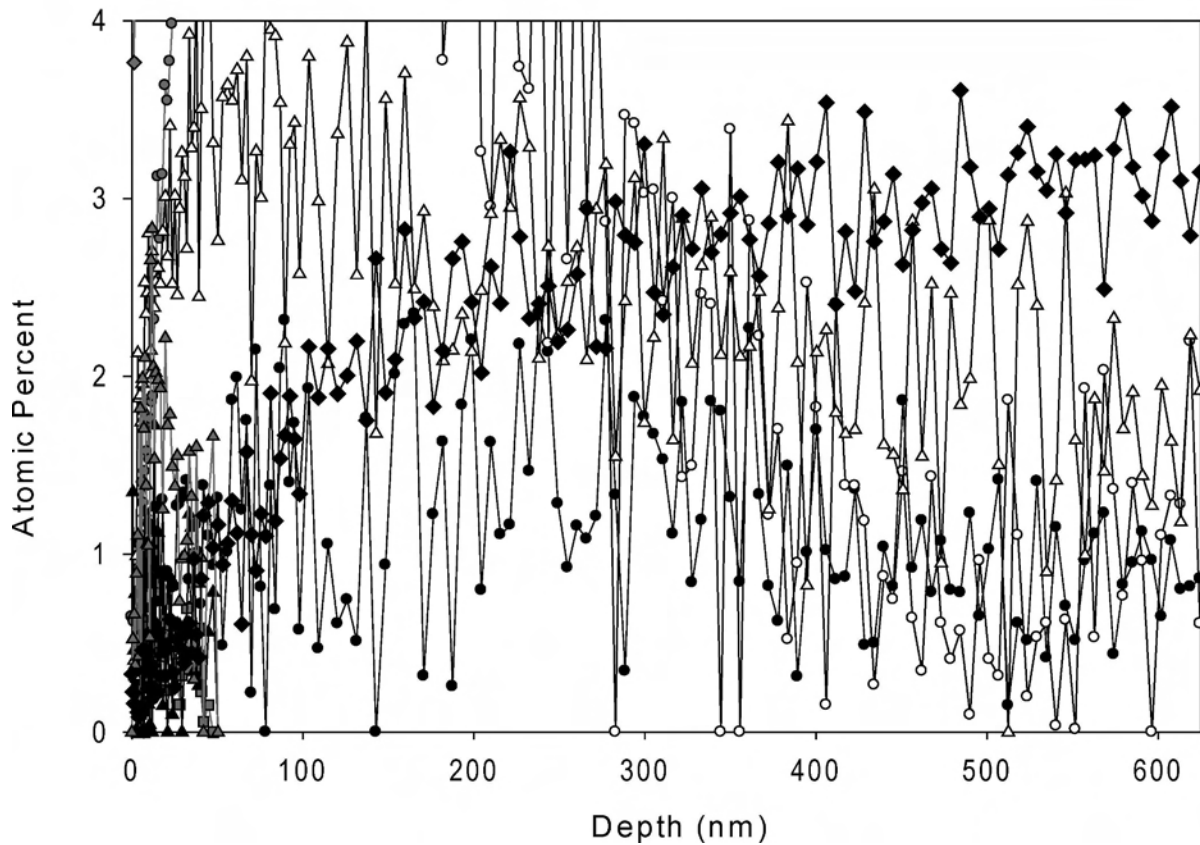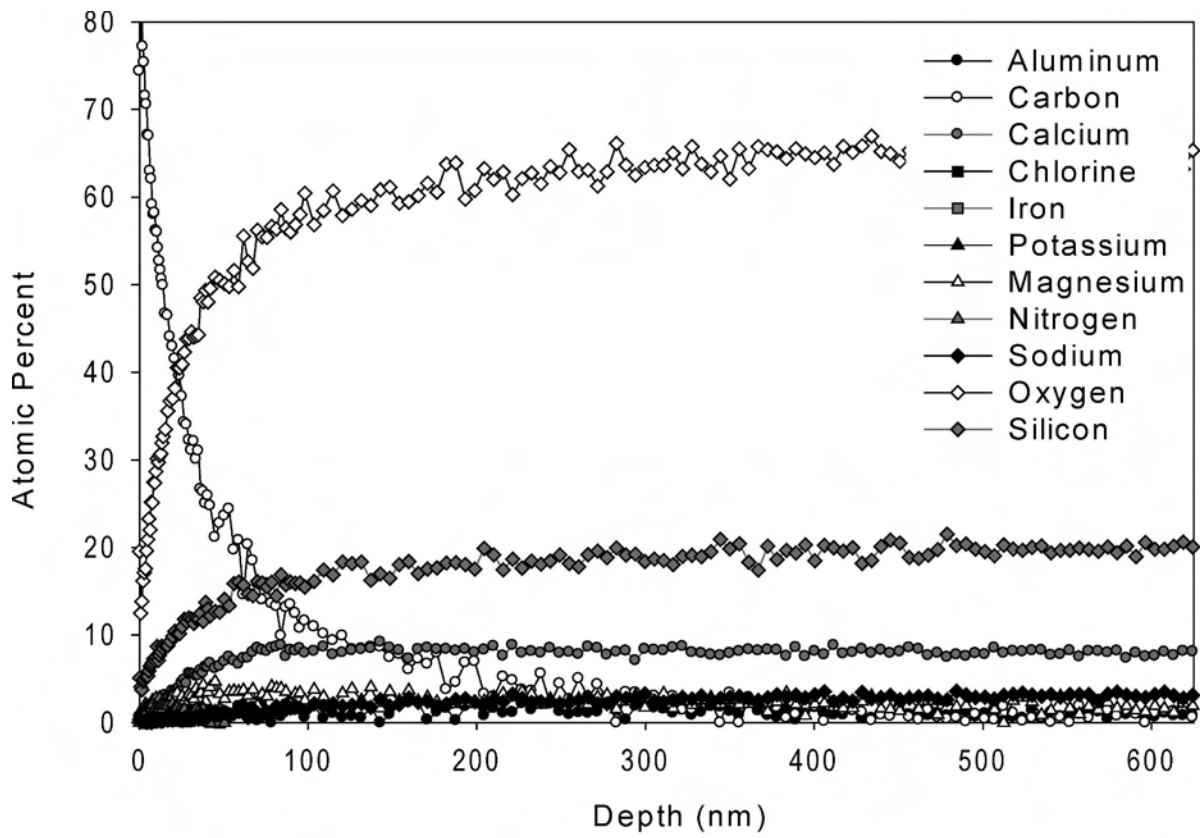
crescentic gouges, and straight grooves, are results of grain-to-grain impacts and abrasion during high-energy subaqueous transport. In contrast, chemical-weathering textures such as c-shaped cracks, halite and silica precipitation, and solution pits occurred during subaerial exposure in the upper foreshore to foreshore–backshore transition zone. Although the sea glass at Port Allen was derived directly from the original source, evidence for chemical overprinting of mechanically formed textures is suggested by well-rounded grains with abundant c-shapes. In the rock record, this overprinting may be erroneously interpreted as a change in depositional environment. The XPS depth profiling shows leaching of Na from the studied glass surfaces. Leach depths appear to vary with glass composition and may be limited by competing mechanical weathering processes.

ACKNOWLEDGMENTS

REFERENCES

BLACKWELDER, P.L., AND PILKEY, O.H., 1972, Electron microscopy of quartz grain surface textures: the U.S. Eastern Atlantic continental margin: Journal of Sedimentary Petrology, v. 42, p. 520–526.

BLAY, C., AND SIEMERS, R., 2004, Kauai's Geologic History: TEOK Investigations, U.S.A., 98 p.

CARTER, C.B., AND NORTON, M.G., 2007. Ceramic Materials: Science and Engineering: New York, Springer Science and Business Media, 716 p.

CHAKROUN, A., MISKOVSKY, J.-C., AND ZAGHBIB-TURKI, D, 2009, Quartz grain surface features in environmental determination of aeolian Quaternary deposits in north-eastern Tunisia: Mineralogical Magazine, v. 73, p. 607–614.

CLAGUE, D.A., 1987, Hawaiian alkaline volcanism, in Filton, J.G., and Upton, B.G.J., eds., Alkaline Igneous Rocks: Geological Society of London, Special Publication 30, p. 227–252.

CLAGUE, D.A., AND DALRYMPLE, G.B., 1987, The Hawaiian–Emperor volcanic chain: Part I, geologic evolution, in Decker, R.W., Wright, T.L., and Stuffer, P.H., eds., Volcanism in Hawaii, U.S. Geological Survey, Professional Paper and Report P-1350, p. 5–73.

CLAGUE, D.A., AND DALRYMPLE, G.B., 1988, Age and petrology of alkali postshield rejuvenated-stage lava from Kauai, Hawaii: Contributions to Mineralogy and Petrology, v. 99, p. 202–218.

CLIFTON, H.E., 1969, Beach lamination—nature and origin: Marine Geology, v. 7, p. 553–559.

DAMIANI, D., GIORGETTI, G., AND TURBANTI, I.M., 2006, Clay mineral fluctuations and surface textural analysis of quartz grains in Pliocene–Quaternary marine sediments from Wilkes Land continental rise (East-Antarctica): paleoenvironmental significance: Marine Geology, v. 226, p. 281–295.

DOREMUS, R.H., 1975, Interdiffusion of hydrogen and alkali ions in a glass surface: Journal of Non-Crystalline Solids, v. 19, p. 137–144.

FLETCHER, R.C., BUSS, H.L., AND BRANTLEY, S.L., 2006, A spheroidal weathering model coupling porewater chemistry to soil thickness during steady-state denudation: Earth and Planetary Science Letters, v. 244, p. 444–457.

FRIDMAN, R.M., 1962, Technology for producing zinc sulfide glass products: Glass and Ceramics, v. 19, p. 444–446.

FRIEDMAN, G.M., ALI, S.A., AND KRINSLEY, D.H., 1976, Dissolution of quartz accompanying carbonate precipitation and cementation in reefs: example from the Red Sea: Journal of Sedimentary Petrology, v. 46, p. 970–973.

HELLAND, P.E., AND HOLMES, M.A., 1997, Surface textural analysis of quartz sand grains from ODP Site 918 off the southeast coast of Greenland suggests glaciations of southern Greenland at 11 Ma: Palaeogeography, Palaeoclimatology, Palaeoecology, v. 135, p. 109–121.

HODEL, K.L., REIMNITZ, E., AND BARNES, P.W., 1988, Microtextures of quartz grains from modern terrestrial and subaqueous environments, north slope of Alaska: Journal of Sedimentary Petrology, v. 58, p. 24–32.

KANEKO, T., 1985, An ion exchange model of glass leaching: Journal of Materials Science, Letters, v. 4, p. 631–634.

KRINSLEY, D.H., AND DORRNKAMP, J.C., 1973. Atlas of quartz sand surface textures: Cambridge University Press, New York, 91 p.

LAMBERT, C.S., 2001. Sea glass chronicles, whispers from the past: Down East Books, Maine, 96 p.

LAMOTTE, R., 2004. Pure Sea Glass: Chesapeake Seaglass Publishing: Maryland, 224 p.

LEBDEVA, M.I., FLETCHER, R.C., BALASHOV, V.N., AND BRANTLEY, S.L., 2007, A reactive diffusion model describing transformation of bedrock to saprolite: Chemical Geology, v. 244, p. 624–645.

MACDONALD, G.A., DAVIS, D.A., AND COX, D.C., 1960, Geology and ground-water resources of the island of Kauai, Hawaii: Hawaii Division of Hydrography, Bulletin 13, 212 p.

MAHANEY, W.C., 2002. Atlas of Sand Grain Surface Textures and Applications: Oxford, U.K., Oxford University Press, 256 p.

MAHANEY, W.C., AND KALM, V., 1995, Scanning electron microscopy of Pleistocene tills in Estonia: Boreas, v. 24, p. 13–29.

MAHANEY, W.C., CLARIDGE, G., AND CAMPBELL, I., 1996, Microtextures on quartz grains in tills from Antarctica: Palaeogeography, Palaeoclimatology, Palaeoecology, v. 121, p. 89–103.

MAHANEY, W.C., VORTISCH, W., AND JULIG, P.J., 1988, Relative differences between glacially crushed quartz transported by mountain and continental ice: some examples from North America and East Africa: American Journal of Science, v. 288, p. 810–826.

MARGOLIS, S.V., AND KENNETT, J.P., 1971, Cenozoic paleoglacial history of Antarctica recorded in subantarctic deep-sea cores: American Journal of Science, v. 271, p. 1–36.

MARGOLIS, S.V., AND KRINSLEY, D.H., 1971, Submicroscopic frosting on eolian and subaqueous quartz sand grains: Geological Society of America, Bulletin, v. 82, p. 3395–3406.

MARGOLIS, S.V., AND KRINSLEY, D.H., 1974, Processes of formation and environmental occurrence of microfeatures on detrital quartz grains: American Journal of Science, v. 274, p. 449–464.

MAZZULLO, J., AND RITTER, C., 1991, Influence of sediment source on the shapes and surface textures of glacial quartz sand grains: Geology, v. 19, p. 384–388.

MIDDLETON, A.P., FREESTONE, I.C., AND LEESE, M.N., 1985, Textural analysis of ceramic thin sections: evaluation of grain sampling procedures: Archaeometry, v. 27, p. 64–77.

MORAL CARDONNA, J.P., GUTIERREZ MAS, J.M., SANCHEZ BELLON, A., LOPEZ-AGUAYO, F., AND CABALLERO, M.A., 1997, Provenance of multicycle quartz arenites of Pliocene age at Arcos, southwestern Spain: Sedimentary Geology, v. 112, p. 251–261.

PATZERT, W.C., AND WYRTKI, K., 1974, Anticyclonic flow around the Hawaiian Islands indicated by current meter data: Journal of Physical Oceanography, v. 4, p. 673–676.

REINERS, P.W., NELSON, B.K., AND IZUKA, S.K., 1999, Structural and petrologic evolution of the Lihue Basin and eastern Kauai, Hawaii: Geological Society of America Bulletin, v. 111, p. 674–685.

SHERROD, D.R., SINTON, J.M., WATKINS, S.E., AND BRUNT, K.M., 2007, Geologic map of the State of Hawaii: U.S. Geological Survey, Open-File Report 2007–1089.

XIE, S.-P., LIU, W.T., LIU, Q., AND NONAKA, M., 2001, Far-reaching effects of the Hawaiian Islands on the Pacific Ocean atmosphere: Science, v. 292, p. 2057–2060.

YANG, Y., MA, J., AND XIE, S.-P., 2008, Observations of the trade wind wakes of Kauai and Oahu: Geophysical Research Letters, v. 35, 5 p.